STEPWISE CARBOTHERMAL REDUCTION OF BAUXITE ORES

[1]Chung Hung Yeh, [2]Guangqing Zhang

[1]School of Materials Science and Engineering, the University of New South Wales, Sydney, NSW 2052, Australia
[2]School of Mechanical, Materials & Mechatronic Engineering, University of Wollongong, Wollongong, NSW 2522, Australia. Email: gzhang@uow.edu.au

ABSTRACT

The commercial technologies for aluminium production include production of alumina from bauxite and smelting of alumina to produce aluminium. The current technology is energy intensive, a major source of greenhouse gas emissions and harmful fluoride emissions. Carbothermal reduction of bauxite is a promising alternative technology for aluminium and aluminoalloy production. Western Australia and Queensland bauxite ores were carbothermally reduced in steps in argon. Experiments were performed in a high temperature vertical tube furnace, and the off-gas composition was monitored using an infra-red gas analyser. The phase composition of reduced samples was characterised by XRD. Oxygen and carbon contents in reduced samples were determined by LECO analysers. The morphology of the surface and intersections was observed by SEM. The chemical compositions of the phases in the reduced samples were detected by EDS. The results of this study have proved the concept of stepwise reduction of bauxite ores in solid state by appropriate control of reduction temperature. Below 1100°C, only iron oxides were reduced to metallic iron. A ferroalloy phase was formed at 1200°C and above. The products in the bauxites reduced to 1600°C include ferroalloy of silicon and aluminium, carbides of titanium, silicon and aluminium, and unreacted alumina.

***KEYWORDS**: Bauxite ores, carbothermal reduction, stepwise reduction, aluminoalloy, aluminium.*

1. INTRODUCTION

The commercial technologies for aluminium production include production of alumina from bauxite and smelting of alumina to produce aluminium. The current technology is energy intensive, a major source of greenhouse gas emissions and harmful fluoride emissions.

Carbothermal reduction of alumina is a promising alternative technology for aluminium and aluminoalloy production. Compared with the Hall-Heroult process, carbothermal reduction of alumina offers advantages of a simpler process, lower cost and a lower requirement for raw materials. Previous assessments showed that carbothermal reduction has the potential to reduce energy consumption by up to 38%, capital costs by more than 60% and decrease CO_2 emissions by up to 30%. It has no any fluoride emission, and may decrease overall operating costs by 25-30% [1-3]. In most works on development of carbothermal reduction of alumina, the strategy of two stage reactors was adopted [4-8]. In these works, an alumina-aluminium carbide melt is first formed, then aluminium is produced from the melt. A technical and economic assessment of the process was presented by Choate and Green [9]. Because of the corrosion/erosion effects of the melt at high temperatures, generally over 2000°C, there are engineering issues in commercialisation of these processes.

Li et al. [10] demonstrated that alumina can be carbothermally reduced in solid phase to form aluminium carbide. The latter can be decomposed to produce aluminium. This suggests a new

potential technology of aluminium production by carbothermal reduction – decomposition.

Production of alumina from bauxite ores consumes a large amount of caustic soda, and generates a large amount of slurry waste "red mud". A desirable process for aluminium production is to start from bauxite in which the impurities, oxides of iron, silicon and titanium can be converted into useful products. Investigations on direct reduction of bauxite are limited in literature. Fujishige et al. [11, 12] investigated the effects of addition of CaO and other Ca containing compounds on the reduction of bauxite in a blast furnace. CaO and $CaCO_3$ addition promotes formation of an aluminium alloy by decreasing the formation of aluminium volatiles. Bauxite with high Fe and low SiO_2 content was considered to be the favourable raw material for aluminium in a blast furnace. Wang et al. [13] patented a technology to reduce bauxite flotation tailings in an electric arc furnace in order to produce a high aluminium alloy at 2300-2500°C. They also reported the formation of an Al-Si alloy at temperatures above 1800°C. They further claimed that the optimum conditions for Al-Si alloy production are: a pressure at 0.1 MPa, a temperature of 1900°C, a carbon content of 95% of the theoretical amount, and one hour heating [14].

Goldin et al. [15] proposed vacuum carbothermal processing of low-iron bauxites. Reduction by dry firing produces ceramic products containing oxide, carbide, and oxycarbide of aluminium, silicon and titanium. Kitajima and Kasai [16] and Mishra et al. [17] investigated processing of the waste red mud from the Bayer process to recover value added products. The former investigation tested the recovery of the iron value by carbothermal reduction. They claimed an achievement of 90% iron recovery by adding $CaCO_3$ as an iron grain coalescence agent. Mishra et al. attempted recovery of alumina in red mud by soda ash sintering and caustic leaching, and iron recovery by carbothermal reduction. The present research investigates carbothermal reduction of bauxite with the major aim to demonstrate the feasibility of reducing bauxite ores at solid state. Both temperature programmed reduction (temperature is ramped continuously with time) and stepwise reduction (where temperature is changed in steps) procedures are used in this work.

2. EXPERIMENTAL

The major compositions of Western Australia and Queensland bauxite ores are presented in eable 1. Western Australia bauxite comprised approximately 40% alumina, 19% iron oxides, 17% silica and ~1% of titania. Compared with Western Australia bauxite, the most significant differences of Queensland bauxite are the alumina and silica contents. Queensland bauxite consists of more than 50% of alumina, 13% iron oxides and 6% silica. Titania content is 2.6% in Queensland bauxite.

Table 1: Major components of bauxites by XRF, wt%

Ore	Al_2O_3	Fe_2O_3	SiO_2	TiO_2
Western Australia Bauxite	39.9	19.3	17.3	1.3
Queensland Bauxite	52.5	13.6	6.5	2.6

Both bauxite ores were reduced carbothermally in flowing argon at 1000 ml/min. The ores were crushed and sieved to < 212 μm and then wet mixed with graphite powder (< 20 μm) in a C/O molar ratio of 1.2:1. After drying, the mixtures were pressed into cylindrical pellets of 8 mm in diameter and about 10 mm in height. Each pellet had a mass of about 1 g. Experiments were performed in a high temperature vertical tube furnace, with a reactor setup presented previously [18]. The off-gas composition was monitored using an infra-red gas analyser. The phase composition of reduced samples was characterised by XRD. Oxygen and carbon contents in the reduced samples were determined by LECO analysers. The morphology of the surface and

intersections was observed by SEM. The chemical compositions of the phases in the reduced samples were detected by EDS.

Temperature programmed reduction experiments were carried out from 850°C until 1600°C, and then the temperature was maintained for 30 min. The rate of reduction as presented by CO evolution rate consisted of multiple peaks. In the step by step reduction experiments, reduction temperatures were decided on the basis of the peak temperatures of reduction curves of the temperature programmed reduction. For Western Australia bauxite, 980°C, 1032°C, 1360°C and 1600°C, and for Queensland bauxite, 1051°C, 1255°C and 1600°C were selected as the step temperatures. The last temperature, 1600°C, was limited by the maximum operation temperature of the furnace used.

3. RESULTS AND DISCUSSION

Western Australia and Queensland bauxite ores were reduced using two reduction procedures. Temperature programmed reduction was followed by sample characterisation to identify the stages of reduction of different metal oxides and their temperature ranges of reduction. Further reduction experiments were carried out in different steps with each step being at constant temperature. This was to further demonstrate the feasibility of stepwise reduction of metal oxides from bauxite ores.

3.1. Progress of Carbothermal Reduction

Temperature programmed reduction was carried out under a flowing argon gas atmosphere. The rate of reduction was monitored by detection of CO released from the reactions using a $CO/CO_2/CH_4$ infra-red analyser.

Figure 1 presents the change of CO content in the off gas during experiments for both bauxites. The reduction curves consist of multiple overlapped peaks, showing that the metal oxides in the bauxite ores were reduced in different temperature ranges. The reduction curve of Western Australia bauxite is more complex than that of Queensland bauxite due to more impurities in the former ore.

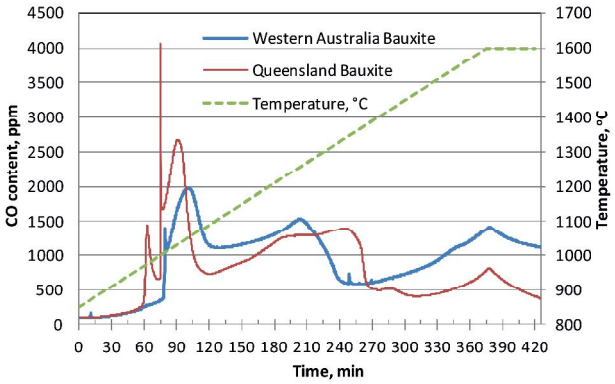

Figure 1: Change in CO content in the off-gas during temperature programmed reduction of bauxite ores. Temperature was ramped from 850 °C to 1600°C at 2°C/min

Based on the major compositions (table 1) and the reducibility of the metal oxides [10, 19-21], it is expected that the first major reduction stage was reduction of iron oxides which took place in the temperature range of 850 to 1100°C. The second major stage of reduction corresponding to the reduction of silica and titania, was in the range of 1100 to 1500°C. Further reduction was mainly attributed to alumina, which was not complete at the end of experiments.

In the step by step reduction experiments, reduction temperatures were decided making reference to the peak temperatures of reduction curves in figure 1. The temperature and CO evolution curves during reduction of Queensland bauxite are presented in figure 2.

During the first step in the step by step reduction experiments, although the furnace temperature was heated to the designated temperatures in advance, the sample temperature took about 20-30 minutes to become stable. So, at the early stage, the reduction temperature was practically changing, although the temperature was labelled constant in figure 2. Reduction of iron oxides during the first step of reduction formed a sharp peak which decreased gradually when the furnace temperature stabilised at 1051°C. Increasing temperature to 1255°C resulted in formation of another CO peak because the rate of reduction increased according to Arrhenius law. Then, the reaction rate slowed down due to consumption of reactants, and then increased and became slow again due to another step increase of temperature to 1600°C.

Bauxite samples reduced to different temperatures were tested by LECO analysers, and the final extents of reduction, that is removal of oxygen combined with metals as oxides during reduction (percentage), were calculated. Table 2 lists the extent of reduction of both bauxite ores reached at different temperatures in the temperature programmed reduction processes.

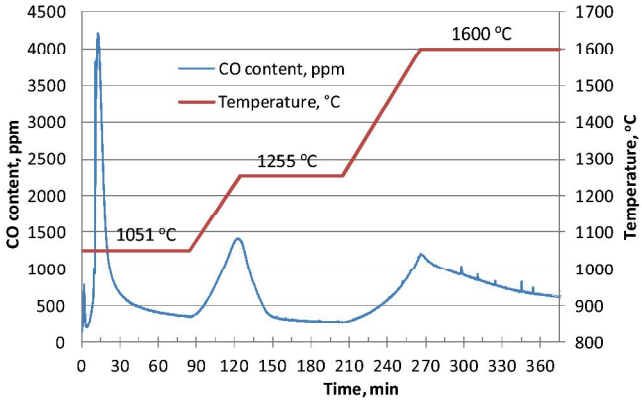

Figure 2: Changes in experimental temperature and CO content in step by step reduction. The ramping rate was 5 °C/min between two step temperatures

Table 2: Extent of reduction of Western Australia and Queensland bauxite ores reduced in argon under different temperatures

Western Australia Bauxite					
Temperature, °C	**1100**	**1300**	**1360**	**1500**	**1600**
Extent of reduction, %	26.8	40.5	43.6	56.1	60.2
Queensland Bauxite					
Temperature, °C	1100	1350	1600		
Extent of reduction, %	17.7	30.9	40.8		

The contribution of each major oxide to the extent of reduction when fully reduced in the two bauxite ores is listed in table 3.

Table 3: Contribution of different metal oxides to the extent of reduction on complete reduction

Metal oxide	**Fe_2O_3**	**SiO_2**	**TiO_2**	**Al_2O_3**
Western Australia bauxite	16.9	26.9	1.5	54.7
Queensland bauxite	12.3	10.3	3.1	74.3

Comparing tables 2 and 3, it can be found that although iron oxide is not completely reduced at 1100°C, the extent of reduction was beyond the maximum possible contribution by Fe_2O_3. So reduction of SiO_2 and TiO_2 occurred at this relatively low temperature, which is a distinct difference from the reduction of the pure oxides.

At 1600°C the extent of reduction for bauxite was also higher than the sum of complete reduction of Fe, Si and Ti oxides. This illustrates partial reduction of alumina took place.

2.2. X-Ray Diffraction (XRD) Analysis

The temperature programmed reduction experiment of Western Australia bauxite (figure 1) was stopped at various temperatures, and the samples reduced to different stages were analysed by XRD. The XRD patterns of reduced samples are presented in figure 3.

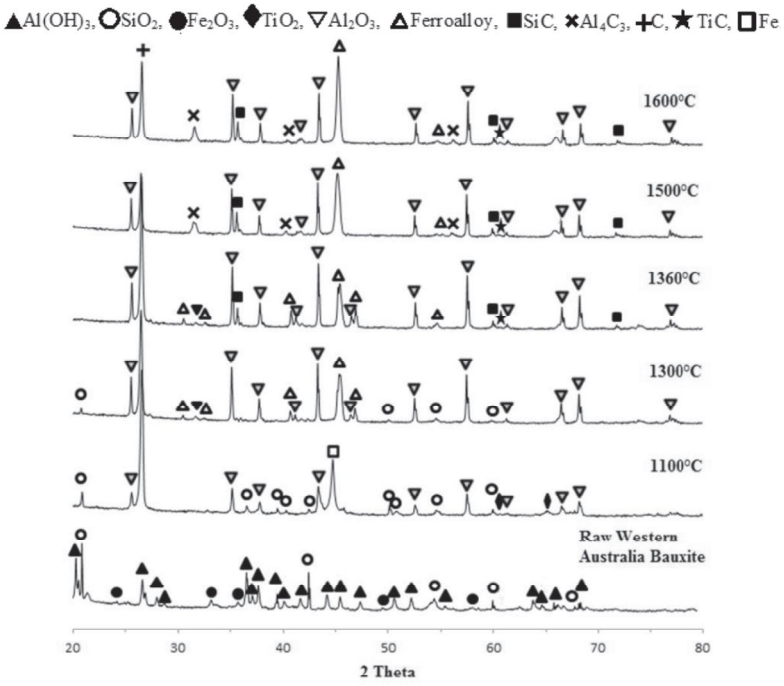

Figure 3: XRD patterns of Western Australia bauxite reduced by temperature programmed reduction to different temperatures

As shown in the figure, original Western Australia bauxite contains hydrated alumina and hematite. Weak peaks of silica were also detected, but not those of titania due to its low content. When the reduction temperature was increased to 1100°C, dehydration of alumina took place, and metallic iron appeared. Weak peaks of titania were also observed. Further reduction to 1300°C made the peaks of alumina stronger, reflecting better crystallisation of alumina. An obvious shift of the iron peak was visible which implies a significant change of its composition, that is, formation of a ferroalloy.

Peaks of SiC were detected in the reduced samples of which the final reduction temperature was 1360°C and above. In the samples reduced until 1500°C and 1600°C, peaks of aluminium carbide, Al_4C_3, were also detected.

Reduction of Queensland bauxite went through a similar route to that of Western Australia bauxite. Raw Queensland bauxite also possesses much hydrated alumina and hematite with small amounts of silica and a trace of titania. Hydrated alumina and hematite converted to alumina and iron metal phase when the temperature rose to 1100°C. Carbides of silicon and titanium were

observed in the samples reduced at 1350°C. Shifting iron peaks indicates that it converts to ferroalloy in the same way as Western Australia bauxite. Peaks of Al_4C_3 appeared in the sample reduced at 1600°C.

In step by step reduction shown in figure 2, experiments were also stopped after each step and the reduced samples were analysed by XRD. When Queensland bauxite was reduced at 1051°C, only hematite converted to metallic iron, which transferred to a ferroalloy phase at 1255°C with reduction of silica (and probably titania). The further reduction until 1600°C caused stronger ferroalloy peak. Oxides stayed in the original phase except Fe_2O_3 at 1051°C. Formation of carbides of silicon and titanium was noted at 1255°C and higher temperatures.

Al_4C_3 is only present in the sample reduced at 1600°C. It is noted that the Al_2O_3 peaks at 1600°C are slightly weaker than the peaks at 1255°C. This demonstrates that significant amount of alumina was reduced with formation of Fe-Si-Al alloy and Al_4C_3.

In the case of Western Australia bauxite, the first step was at 980°C at which only hematite was reduced. Further reduction to 1032°C made the peaks of iron stronger. At 1360°C, new peaks appeared, included those of SiC and TiC. Moreover, the better crystallization of Al_2O_3 gave stronger Al_2O_3 peaks, and a ferroalloy phase was also detected. Up to 1600°C reduction, the peak of ferroalloy phase became very strong. Al_4C_3 peaks also appeared at 1600°C.

3.3. Scanning Electron Microscope (SEM) Analysis of Reduced Samples

Figure 4 shows the BSE image and the EDS spectra of two different phases in a Western Australia bauxite sample reduced up to 1600°C and further reduced at the temperature for two hours. From figure 4(a), the reduced bauxite sample is with a porous structure. The dark gray zones are pores which are presented as carbon in composition by EDS analysis. According to figure 4 (b) and (c), the bright zones in the BSE image are metallic phase of iron, silicon and aluminium, while the light gray phase contains mainly alumina with very small level of iron oxide. The detected elemental compositions of the reduced sample at the two points marked in figure 4 are presented in table 4. The content of carbon is not correct in this analysis because the sample was coated with carbon before analysis.

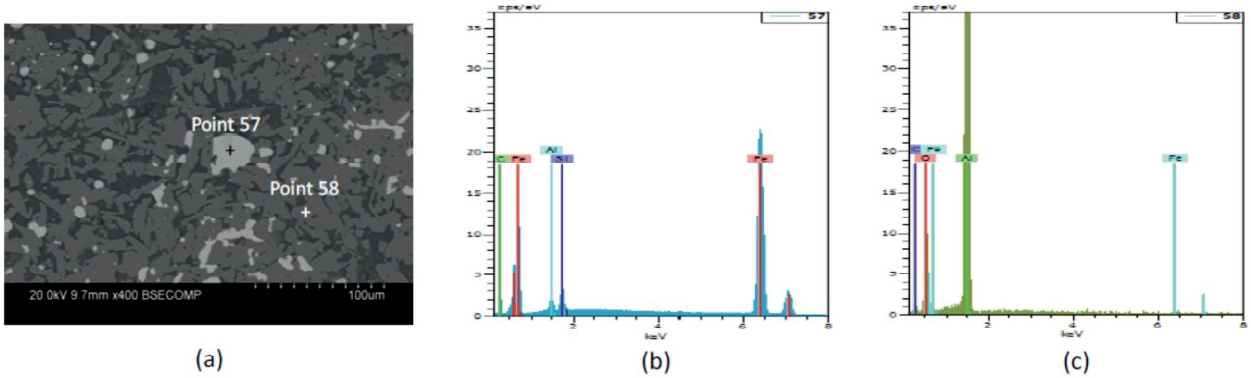

Figure 4: SEM and EDS analyses of a sample of Western Australia bauxite reduced at 1600°C. (a) BSE image; (b) EDS spectrum at point 57; (c) EDS spectrum at point 58

From the morphology of the bauxite particle, the oxide phase was not melted at the final temperature of reduction up to 1600 °C. This means that only the metallic phase (ferroalloy) is melted during reduction which is distributed in the solid oxide matrix. So, solid phase carbothermal reduction of bauxite ores can be achieved by stepwise reduction of metal oxides without forming a molten slag.

Table 4: Elemental composition of phases marked in figure 4(a)

Point 57				Point 58			
Element	**wt%**	**Normalised wt%**	**Normalised at%**	**Element**	**wt%**	**Normalised wt%**	**Normalised at%**
Fe	64.9	82.6	53.8	O	40.5	43.7	51.7
C	10.7	13.6	41.2	Al	41.9	45.3	31.7
Si	1.8	2.3	3.0	C	9.7	10.4	16.4
Al	1.2	1.5	2.0	Fe	0.6	0.6	0.2
Sum	78.6	100.0	100.0	Sum	92.7	100.0	100.0

Figure 5 presents a BSE image and EDS elemental distribution of a Western Australia bauxite sample reduced to 1600°C. The big bright grain in the BSE image is Fe-Si-Al alloy. The existence of silicon in the ferroalloy phase is obvious in the EDS image. However, a contour of aluminium in the alloy phase is not demonstrated due to its low content in comparison with that in the oxide phase (high in alumina). The gray inclusions within the alloy grain are aluminium oxide. This aluminium oxide phase was supposed to be from hydrolysis of Al_4C_3 when the sample was exposed to the moisture in air or during preparation of the sample for SEM analysis. Titanium bright dots are distributed around and within the grain, which do not correspond to high oxygen content. It is supposed that this titanium is in carbide. TiC does not have high solubility in ferroalloy phase. Titanium oxides were reduced into titanium dissolved in the ferroalloy phase at high temperatures. During cooling, titanium is segregated and combined with carbon to form TiC.

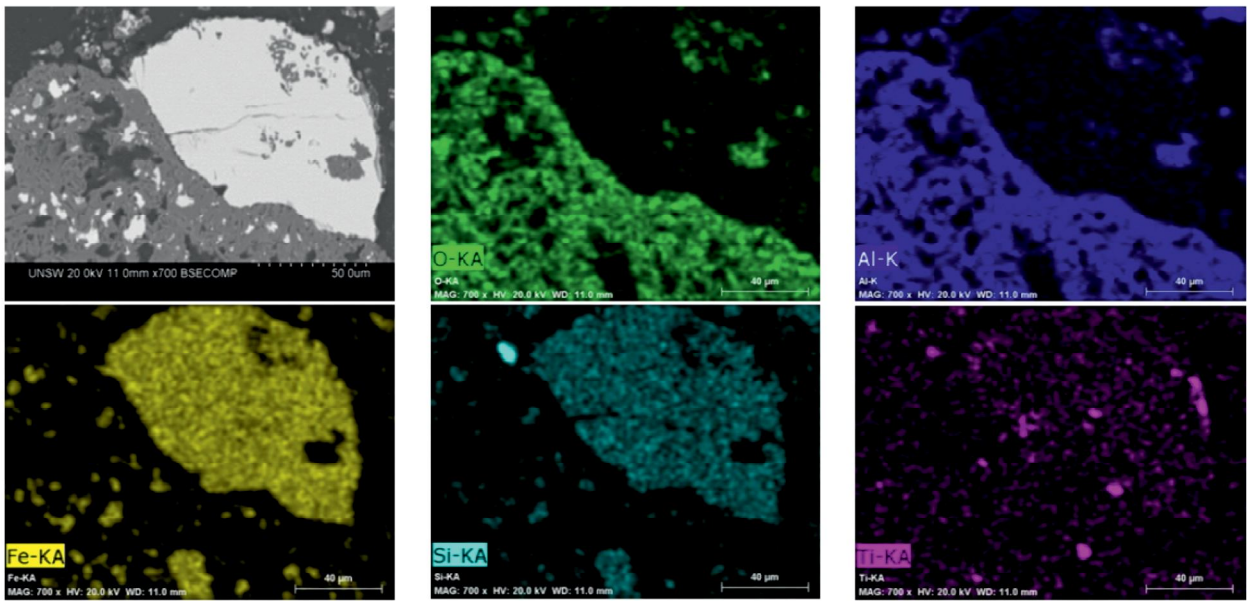

Figure 5: BSE image and EDS elemental distribution of Western Australia bauxite ore reduced up to 1600°C

Figure 6 presents a BSE image and the EDS elemental distribution of a Queensland bauxite sample reduced to 1600°C. SiC grains are included in ferroalloy matrix and beside the ferroalloy. These SiC grains were formed by segregation from ferroalloy phase during cooling. The growth of SiC grains broke the alloy grain into pieces or formed fractures. Segregated small TiC grains from the ferroalloy phase are also observed within and around the ally grain.

Al_2O_3, TiO_2 and SiO_2 are stable oxides difficult to reduce. Solid state carbothemal reduction of these pure oxides is through gas phase. However, carbothermal reduction of these oxides from bauxite ores in the presence of molten iron from reduction of iron oxides may become easier: carbon as a reductant can be transferred via the liquid metal phase from graphite to the oxides. Formation of ferroalloy phase by metallic aluminium, silicon and titanium decreases their activities so that their reduction becomes more favourable until the ferroalloy phase becomes saturated with corresponding carbides.

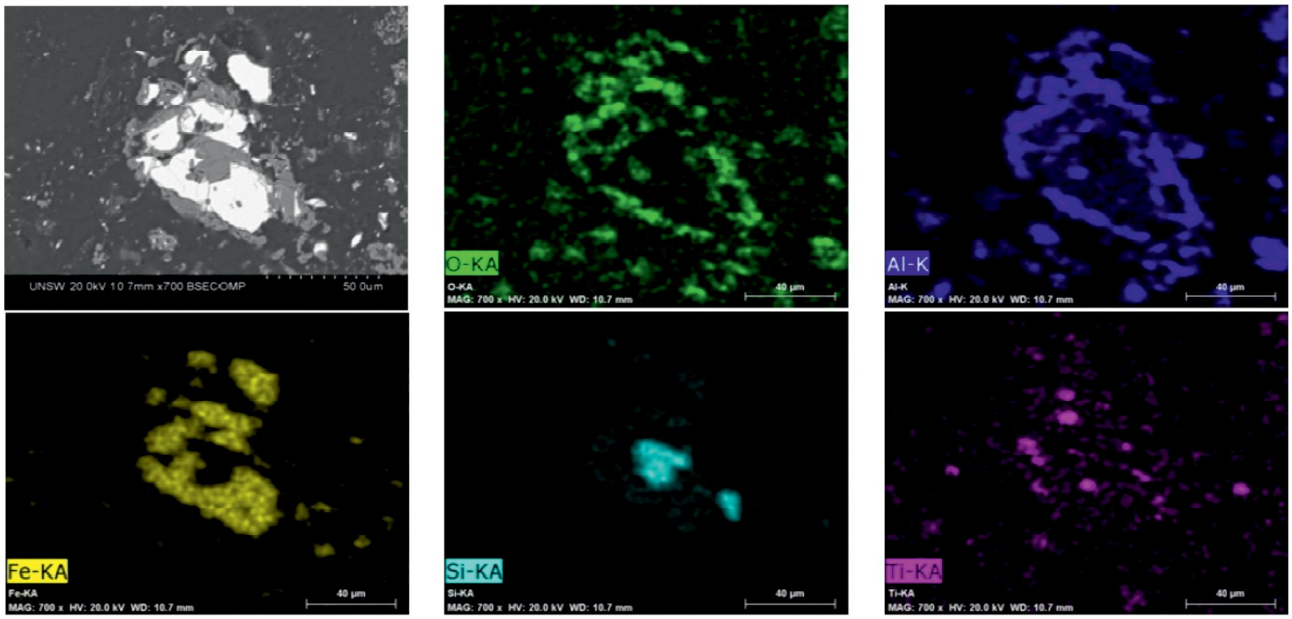

Figure 6: BSE images and EDS elemental distribution of Queensland bauxite reduced up to 1600°C

4. CONCLUSIONS

The carbothermal reduction of bauxite ores from Western Australia and Queensland was carried out in Ar atmosphere, using temperature programmed reduction and step by step reduction procedures. The major conclusions of this research are:

(1)Bauxite ore can be directly reduced carbothermally by temperature programmed reduction or stepwise reduction process. Appropriate control of reaction temperature may maintain the residual oxide phases in solid state.

(2)The reduction sequence of the metal oxides in the bauxite ores is iron oxides then silica and titania and then alumina. Metallic iron is formed at temperatures below 1100°C. At 1200°C or above a ferroalloy phase with silicon and aluminium is formed.

(3) Carbides of titanium, silicon and aluminium were formed by carbothermal reduction. The metals were formed and dissolved in the ferroalloy phase, which upon saturation, were segregated as metal carbides distributed inside alloy phase as inclusions or around the alloy particles.

5. REFERENCES

[1] M.J. Bruno, Light Metals 2003 (Ed. P.N. Crepeau), TMS (The Minerals, Metals & Materials Society), 2003, 395-400.

[2] Y. Sayad-Yaghoubi, Patent WO 2007012123, 2007, 19 pp.

[3] H. Myklebust and P. Runde, Light Metals 2005, 519-522.
[4] E. Gruenert and J. Mercier, Patent DE 1144014, 1963, 3pp. 4) C. N. Cochran and N. M. Fitzgerald: Patent US, 4299619, (1981).
[5] J. A. Persson, Patent US 4385930, 1983, 5pp.
[6] P. D. Dougan and F. W. Southam, Patent CA 1184390, 1985, 7pp.
[7] V. A. Dmitriev and S. V. Karasev, Patent RU 2157856, 2000.
[8] K. Johansen, J. A. Aune, M. Bruno, and A. Schei, Light Metals 2003 (Ed. P.N. Crepeau), TMS (The Minerals, Metals & Materials Society), 2003, 401-406.
[9] W. Choate and J. Green, Light Metals 2006, 445-450.
[10] J. Li, G. Zhang, D. Liu, and O. Ostrovski, ISIJ International, 2011, 51(6), 870-877.
[11] M. Fujishige, H. Yokokawa, S. Ujiie and M. Dokiya, Kagaku Gijutsu Kenkyusho Hokoku, 1986, 81(12), 731-736.
[12] M. Fujishige, H. Yokokawa, S. Ujiie and M. Dokiya, Nippon Kinzoku Gakkaishi, 1986, 50(8), 727-734.
[13] Y. Wang, N. Feng, J. You and J. Peng, Faming Zhuanli Shenqing, Patent CN 101632958 A, 2010.
[14] D. Yang, N. Feng, Y. Wang and X. Wu, Trans. Non-ferrous Met. Soc. China, 2010, 20, 147-152.
[15] B. A. Goldin, V. E. Grass and Yu. I. Ryabkov, Glass and Ceramics, 1999, 55(9-10), 323-325.
[16] T. Kitajima and E. Kasai, Shigen to Sozai, 1999, 115(8), 611-617.
[17] B. Mishra, A. Staley, D. Kirkpatrick, Miner. Metall. Process., 2002, 19(2), 87-94.
[18] G. Zhang and O. Ostrovski, Metall. Mater. Trans. B, 2000, 31B, 129-139.
[19] M. Dewan, G. Zhang, and O. Ostrovski, Metall. Mater. Trans. B, 2009, 40B (1), 62-69.
[20] M. A. R. Dewan, G. Zhang, and O. Ostrovski, Metall. Mater. Trans. B, 2010, 41B(1), 182-192.
[21] M. A. R. Dewan, G. Zhang, and O. Ostrovski, Inst. Min. Metall. Trans. C: Miner. Process. Extr. Metall., 2011, 120 (2), 111-117.